AIMS Mathematics, 7(5): 8510–8533.
DOI: 10.3934/math.2022474
Received: 12 December 2021
Revised: 15 February 2022
Accepted: 16 February 2022
Published: 28 February 2022

http://www.aimspress.com/journal/Math

Research article

Thermoelastic reactions in a long and thin flexible viscoelastic cylinder due to non-uniform heat flow under the non-Fourier model with fractional derivative of two different orders

Ahmed Abouelregal[1,2,*], Meshari Alesemi[3] and Husam Alfadil[1]

[1] Department of Mathematics, College of Science and Arts, Al-Qurayyat, Jouf University, Saudi Arabia
[2] Basic Sciences Research Unit, Jouf University, Saudi Arabia
[3] Department of Mathematics, College of Science, University of Bisha, Bisha, Saudi Arabia

* **Correspondence:** Email: ahabogal@ju.edu.sa; Tel: +966531059740; Fax: +9660146432032.

Abstract: In this paper, a new fractional model of non-Fourier heat conduction is presented that includes phase delays and two fractional orders. To derive the proposed model, the fractional integral Atangana-Baleanu (AB) operator with non-singular and non-local kernels was used. The proposed model has been applied to solve a one-dimensional thermoelasticity problem that includes an annular cylinder of a flexible material whose inner and outer surfaces are subjected to a variable heat flux that depends on time and temperature and is free from traction. The Laplace transform approach was applied to find the general solution to the problem and to obtain the expressions for the different physical fields. To estimate the effects of the fractional-order parameters and instantaneous time on the responses of all thermophysical field variables, comparisons are presented in figures and tables.

Keywords: fractional-order; thermoelasticity; annular cylinder; phase delays; Atangana-Baleanu operator
Mathematics Subject Classification: 74A35, 74F05, 80A19, 65M60

1. Introduction

The well-known Fourier law defining the linear dependence between the heat flow vector and the temperature gradient was proposed by Fourier in 1822, which marks the beginning of the classical theory of heat transfer. Fourier's student, Duhamel, pioneered work on thermoelasticity a few decades ago by combining the temperature distribution with the deformation of matter [1]. In some physical conditions, the classical theory of thermal conductivity, derived from Fourier's theoretical law, is well suited but overlooks phenomena that occur at the microscopic level. Numerous theoretical and empirical investigations have shown that the description of transfer processes through the classical Fourier law and the typical parabolic heat transfer equation is no longer reliable in media with complex internal structures. As a result, physical processes at the microscopic level have to be viewed differently from conventional ones [2]. For this reason, new, non-classical models of thermoelasticity have been developed in which Fourier's law and the equivalent heat transfer equation have been replaced by new models that include more general equations.

In the course of developing the classical theory of thermoelasticity, many generalized models have been proposed. To name a few, Lord and Shulman (LS) [3], Green-Lindsay (GL) [4], and Green and Naghdi [5–7] theories. Tzou [8] also introduced two independent phase lag times in the Fourier law of thermal conductivity as an alternative method for developing the classical theory that predicts thermal disturbances' unrestricted propagation velocity. A survey and presentation of ideas generalized in this area can be found at [9]. Also, in the overview paper [10], Hetnarski and Ignaczak investigated five generalizations of the dual model and came to a number of interesting analytical conclusions. Not only that but other attempts and efforts have been made to adapt the traditional Fourier law in order to generalize the previous models using new mathematical models of thermal elasticity that include higher-order time derivatives [11–13].

In the thermal and mechanical sectors, Zhou and Li [14] presented a novel analysis of thermoelastic damping that took into account the non-Fourier heat transfer impact as well as size-dependent influences. Zhou et al. [15] used a non-Fourier model, a single-phase lag model, to develop analytical models for the thermal-elastic damping of rectangular micro-and nano-ring resonators with heat conduction in the radial thickness direction and the creation of the circumferential direction. In recent years, these generalized thermoelastic models optimized for thermal conductivity have been used to investigate several types of thermoelastic problems. Phase-lagging and non-local theories have also been proposed for the size-dependent effect on thermal conductivity [16,17].

The frequent presence of fractional calculus in diverse applications in fluid mechanics, heat conduction, diffusion difficulties, chemical physics, viscoelasticity, and other fields has sparked increased interest in the topic of fractional calculus in recent years. Fractional calculus (also known as fractional order derivatives and integrals) is a useful tool for describing the memory and heredity qualities of many substances. This is the main advantage of fractional order concepts over integer-order models, in which such effects are actually ignored. Abel used fractional calculus to address the integral equation in the construction of the Tautochrone problem, which was the first time he used fractional calculus [18]. Since the solution of some systems predicts an instantaneous reaction when using the regular derivatives, fractional calculus (fractional derivatives) was used to explain viscoelastic materials better than the regular derivatives [19]. Ross [20] and Miller and Ross [21] provided a historical context for the development of fractional calculus. In this context also,

Podlobny [22] provided an overview of a number of additional applications of fractional calculus in fields of science such as physics, engineering, and others.

There are many examples of materials in which the traditional thermoelastic theory has failed, as well as extended thermoelastic models in which the fields have low temperatures, such as glassy, porous materials, synthetic and biological materials, amorphous media, and transient loading. As a result, the inclusion of the concept of fractional derivatives of time in the field of thermoelastic theory is very important in such cases. Povstenko [23] presented a new fractional derivative thermal conductivity model based on the Caputo concept [24] to investigate thermoelastic interactions in an infinitely hollow cylindrical body. Sherief et al. [25] proposed an alternative model based on the fractional calculus of extended thermoelasticity. In the same paper, a reciprocity relation, a uniqueness theorem, and a variational principle are constructed. For example, after the emergence of the concept of fractional thermoelastic models, many interpretations were presented in the field of fractional thermoelasticity as an extension of Lord-Shulman's theory [3], Green-Naghdi models [5–7], and Tzou's theory [8], and the authors had different physical images of this subject [26–34].

Most of the models that have been proposed in the context of fractional calculus are based on the basic concepts introduced by Caputo and Riemann-Liouville. The well-known Caputo and Riemann-Liouville kernels both have a major flaw: they are nonlocal but singular. When simulating real-world problems, this flaw has an impact. Some fractional derivative formulations, such as the Caputo-Fabrizio fractional derivatives, have recently been proposed that are based on non-singular kernels. The Caputo-Fabrizio derivative of the fractional-order is one of the new operators introduced by Caputo and Fabrizio [35]. Some researchers in the field of fractional calculus have concluded that the Caputo-Fabrizio derivative was not a fractional derivative but only a filter with a fractional parameter.

Atangana and Baleanu proposed a new fractional-order operator based on the Mittag-Leffler function [36,37] to meet the challenges mentioned above. Furthermore, their operators offer all of the advantages of Caputo and Fabrizio, and the kernel is nonlocal. The operators have the same advantages as the Riemann-Liouville fractional integral of the provided function and the function itself. In addition to the obvious advantages, the derivative has been proven to be particularly effective in the thermal and material sciences [38]. These novel fractional derivatives are both filters and fractional derivatives [39]. The nonlocal fractional derivative with a non-singular kernel, known as the Atangana-Baleanu derivative, has a wide range of applications [40–45].

The main objective of this paper is to present a new development and application in the field of fractal thermoelasticity involving Atangana and Baleanu fractional derivative operators with non-singular and non-local kernels that are based on the generalized Mittag-Leffler function. The analysis was derived using the dual-phase lag model (DPL) and includes two-order fractional time derivatives. To explain the importance of the proposed fractional heat conduction model, thermoelastic interactions are discussed in an annular cylinder whose surfaces are free of traction and induced by time-dependent oscillating heat. The governing equations in cylindrical coordinates were solved using an analytical approach based on the Laplace transform method. The numerical inversion of expressions for displacement, stress, and temperature in the physical field was found using a given algorithm. The numerical values of the field variables for copper material were calculated. The numerical results are presented in figures and tables for the purpose of making comparisons of physical quantities to investigate the effect of the fractional parameter and the instantaneous time parameter. The current model can also be reduced to some interesting special cases.

Below is a breakdown of the organization of the current paper. The basics of thermoelastic theory and an overview of fractional calculus and its importance are presented in the current section. Section 2 focused on non-local fractional time derivations of Fourier's law based on the Atangana and Baleanu derivative operators. In Section 3, the proposed fractional mathematical model was used to examine thermoelastic interactions in an annular cylinder caused by time-dependent oscillating heat. In the fourth and fifth sections, a straightforward technique is used to solve the problem in the field of Laplace transform and to determine its numerical reflection using the Fourier series expansion methodology. Through figures and tables, Section 6 compares the results obtained, except in the case of the extended and fractional and non-fractional models. In the last section, the most important conclusions and observations obtained from the numerical values and discussions are summarized.

2. Mathematical model of fractional thermoelasticity

In the current section, some of the basics of fractional calculus will be explained. There are several types of integral and differential fractional-order operators. Numerous mathematicians have come up with numerous definitions of an integral or derivative incorrect order over the years, each using their own method and technique. The Riemann-Liouville definition is one of the forms that has gained popularity in the world of fractional calculus and has been in use for decades. For any non-negative real number α ($\alpha \in \mathbb{R}^+$) and for $t > 0$, the Riemann-Liouville fractional integral of the integrable function $f(t)$ has the following form [46]:

$$RLD_t^{\alpha} f(t) = \frac{1}{\Gamma(n-\alpha)} \frac{d^n}{dt^n} \int_0^t \frac{f(\xi)}{(t-\xi)^{\alpha+1-n}} \mathrm{d}\xi, n-1 < \alpha \leq n \in \mathbb{N}, \tag{1}$$

where $\Gamma(\alpha)$ symbolizes the well-known gamma function. In addition, the Caputo derivative of fractional derivative can be expressed as [24]:

$$CD_t^{\alpha} f(t) = \frac{1}{\Gamma(n-\alpha)} \frac{d^n}{dt^n} \int_0^t \frac{f^{(n)}(\xi)}{(t-\xi)^{\alpha+1-n}} \mathrm{d}\xi, n-1 < \alpha \leq n \in \mathbb{N}. \tag{2}$$

Atangana and Balanu proposed a significantly superior version without a singular kernel that addresses the concerns raised by Caputo-Fabrizio [35]. The generalized non-singular and non-local Mittag-Leffler function E_{α} serves as the basis for their derivative. Depending on Caputo's interpretation, the definition of the fractional derivative of Atangana and Baleanu (AB) of the order $\alpha \in (0,1)$ can be written as [45,46]:

$$ABD_t^{(\alpha)} f(t) = \frac{1}{1-\alpha} \int_0^t \frac{\partial f(\xi)}{\partial \xi} E_{\alpha}\left[-\frac{\alpha(t-\xi)^{\alpha}}{1-\alpha}\right] \mathrm{d}\xi, 0 < \alpha \leq 1 \tag{3}$$

The significance of the Laplace transform approach in the study of differential equations is well recognized. It is also recognized that for, $0 < \alpha \leq 1$ for this new fractional definition [47]

$$\mathcal{L}\left[ABD_t^{(\alpha)} f(t)\right] = \frac{s^{\alpha}\mathcal{L}[f(t)] - s^{\alpha-1} f(0)}{s^{\alpha}(1-\alpha)+\alpha}, \ s > 0. \tag{4}$$

As a result, it is evident that the Laplace transform will be helpful when dealing with the Atangana-Baleanu fractional derivative.

The classical Fourier law of heat transfer can be determined by the linear relationship between the heat flow vector $\vec{q}$ and the heat gradient $\nabla\theta$ as:

$$\vec{q} = -K\nabla\theta \tag{5}$$

where K is thermal conductivity, $\theta = T - T_0$ represents the temperature change, and T_0 denotes the reference temperature. The energy conservation law is stated as follows:

$$\frac{\partial}{\partial t}(\rho C_E\theta + \gamma T_0 e) = -\nabla\cdot\vec{q} + Q. \tag{6}$$

The classical parabolic thermal conductivity equation can be obtained by combining Fourier's law (5) with Eq (6). The parabolic heat equation predicts that a thermal signal can be seen at a long distance from its source. From a physical point of view, the heat field with infinite speed is unacceptable. That is why efforts have been made over the past few decades to address the shortcomings of Fourier's law. Several models of non-Fourier heat transfer have been developed, especially those that represent a finite heat diffusion velocity [3–8].

Tzou [8,48,49] proposed a two-phase lag (DPL) model that addresses the issue of instantaneous interaction involving temperature and energy in Fourier's law. The DPL model, in particular, provides an accurate and direct representation of heat transfer in materials, especially in skin tissues. In this model, the conventional Fourier law is replaced by a general relationship between the heat flow vector $\vec{q}$ at any position $\vec{x}$ of the material at time $t + \tau_q$ and the temperature gradient at the same position at time $t + \tau_\theta$, which is described by the relationship

$$\vec{q}(\vec{x}, t + \tau_q) = -K\nabla\theta(\vec{x}, t + \tau_\theta). \tag{7}$$

The symbols τ_q and τ_θ denote the delay times, which are among the intrinsic properties of the material. The heat transfer equation for the DPL model may be expressed as follows using the first-order approximation for both sides of Eq (7):

$$\left(1 + \tau_q\frac{\partial}{\partial t}\right)\vec{q} = -K\left(1 + \tau_\theta\frac{\partial}{\partial t}\right)\nabla\theta. \tag{8}$$

The fractional heat transfer equation better describes heat diffusion in materials with complex internal structures [30]. The present study is an attempt to build a new generalized model of thermoelasticity using the characteristic Atangana-Baleanu (AB) fractional derivative operator. This modification is based on replacing the time derivative in Eq (8) with the fractional derivative AB defined in Eq (3). As a result, the fractional heat conduction equation with the Atangana-Baleanu derivative can be given by:

$$\left(1 + \tau_q ABD_t^{(\alpha)}\right)\vec{q} = -K\left(1 + \tau_\theta ABD_t^{(\alpha)}\right)\nabla\theta, 0 < \alpha \leq 1. \tag{9}$$

In the models that have been proposed in this context, the researchers in their study did not take into account the energy equation of change even though they made significant advances using Fourier's theorem. In this work, another improvement will be made in this extension, not through Fourier's law, but through a change in the energy equation (6). In the energy equation (6), the time

derivative will be replaced by a fractional derivative with a new different order β. In this modification, the energy equation restructured into fractional order β will take the following form [50]:

$$\tau_1^{\beta-1} ABD_t^{(\beta)}(\rho C_E \theta + \gamma T_0 e) = Q - \nabla \cdot \vec{q}, 0 < \beta \leq 1. \tag{10}$$

The parameter $\tau_1^{\beta-1}$ in the above equation is used to maintain dimensional consistency. The following fractional heat transfer equation can be obtained by combining equation (9) with the modified fractional energy equation (10):

$$\begin{aligned}\left(1 + \tau_q ABD_t^{(\alpha)}\right)\left(\rho C_E \tau_1^{\beta-1} ABD_t^{(\beta)}\theta + \gamma T_0 \tau_1^{\beta-1} ABD_t^{(\beta)} e\right) \\ = K\left(1 + \tau_\theta ABD_t^{(\alpha)}\right)\nabla^2\theta - \left(1 + \tau_q ABD_t^{(\alpha)}\right)Q\end{aligned}. \tag{11}$$

Moreover, for a thermo-isotropic solid, the constitutive relations, stress-displacement relations and the equation of motion are as follows:

$$\sigma_{ij} = \lambda \delta_{ij} e_{ij} + 2\mu e_{ij} - \gamma\theta\delta_{ij} \tag{12}$$

$$2e_{ij} = \frac{1}{2}\left(u_{i,j} + u_{j,i}\right) \tag{13}$$

$$\mu u_{i,jj} + (\lambda + \mu) u_{j,ij} - \gamma\theta_{,i} + F_i = \rho\ddot{u}_i. \tag{14}$$

The complete set of equations that govern the theory of thermoelasticity of the fractional order consists of Eq (11) to Eq (14).

3. Special cases

3.1. Fractional thermoelastic model with Atangana-Baleanu (AB) operator (1FABTE)

The thermal conductivity equation can be obtained using the AB fractional derivative operator and a single fractional order as a limited case when $\beta \to 1$. In this case, we have

$$\left(1 + \tau_q ABD_t^{(\alpha)}\right)\left(\rho C_E \frac{\partial\theta}{\partial t} + \gamma T_0 \frac{\partial e}{\partial t}\right) = K\left(1 + \tau_\theta ABD_t^{(\alpha)}\right)\nabla^2\theta + \left(1 + \tau_q ABD_t^{(\alpha)}\right)Q. \tag{15}$$

3.2. Fractional dual-phase lag model proposed by Ezzat et al. (FEDPL) [51]

The fractional DPL heat transfer model proposed by Ezzat [51] taking into account the Riemann-Liouville fractional integral can be obtained from Eq (11) when $\beta \to 1$ and $\tau_q = \frac{t_q^\alpha}{\alpha!}$ and $\tau_\theta = \frac{t_\theta^\alpha}{\alpha!}$

$$\left(1 + \frac{t_q^\alpha}{\alpha!}\frac{\partial^\alpha}{\partial t^\alpha}\right)\left(\rho C_E \frac{\partial\theta}{\partial t} + \gamma T_0 \frac{\partial e}{\partial t}\right) = \left(1 + \frac{t_\theta^\alpha}{\alpha!}\frac{\partial^\alpha}{\partial t^\alpha}\right)\nabla^2\theta + \left(1 + \frac{t_q^\alpha}{\alpha!}\frac{\partial^\alpha}{\partial t^\alpha}\right)Q. \tag{16}$$

3.3. Fractional model with single-phase lag proposed by Sherief et al. (FSLS) [25]

The fractional heat transfer model with single-phase lag proposed by Sherief et al. (FSLS) [25]

taking into account the Riemann-Liouville fractional integral can be obtained from Eq (11) when putting the parameter $\tau_\theta = 0$ and $\beta \to 1$

$$\left(1 + \tau_q \frac{\partial^\alpha}{\partial t^\alpha}\right)\left(\rho C_E \frac{\partial \theta}{\partial t} + \gamma T_0 \frac{\partial e}{\partial t}\right) = \left(1 + \tau_\theta \frac{\partial^\alpha}{\partial t^\alpha}\right)\nabla^2\theta + \left(1 + \tau_q \frac{\partial^\alpha}{\partial t^\alpha}\right)Q. \tag{17}$$

3.4. Dual-phase lag model of thermoelasticity (DPL) [8]

The DPL heat transfer model can be obtained from Eq (11) when $\beta \to 1$ and $\alpha \to 1$.

$$\left(1 + \tau_q \frac{\partial}{\partial t}\right)\left(\rho C_E \frac{\partial \theta}{\partial t} + \gamma T_0 \frac{\partial e}{\partial t}\right) = \left(1 + \tau_\theta \frac{\partial}{\partial t}\right)\nabla^2\theta + \left(1 + \tau_q \frac{\partial}{\partial t}\right)Q. \tag{18}$$

3.5. Lord-Shulman thermoelastic model (LS) [3]

The LS heat transfer model with single-phase lag can be obtained from Eq (11) by putting $\tau_\theta = 0$ and taking $\alpha, \beta \to 1$.

$$\left(1 + \tau_q \frac{\partial}{\partial t}\right)\left(\rho C_E \frac{\partial \theta}{\partial t} + \gamma T_0 \frac{\partial e}{\partial t}\right) = \nabla^2\theta + \left(1 + \tau_q \frac{\partial}{\partial t}\right)Q. \tag{19}$$

3.6. Classical thermoelasticity theory (CTE)

Heat equation (11) reduces to the classical heat equation (CTE) when $\tau_q = \tau_\theta$ and $\beta, \alpha \to 1$

$$C_E \frac{\partial \theta}{\partial t} + \gamma T_0 \frac{\partial e}{\partial t} - Q = K\nabla^2\theta. \tag{20}$$

4. Application and problem formulation

To analyze and verify the new model, we will consider a boundary value problem. The vibration of thermoelastic material will be studied in a hollow cylinder with an inner radius of r_1 and an outer radius of r_2, respectively (see Figure 1). The following assumptions about the initial boundary and boundary constraints of the proposed problem are considered:

- Hollow cylinder surfaces are not exposed to any external heat sources or body forces.
- The initial conditions are intended to be quiet.
- Hollow cylinder surfaces are traction-free.
- Hollow cylinder surfaces are exposed to either a time-dependent or constant ambient temperature.

A cylindrical system of polar coordinates (r, ϕ, z) will be employed. The problem is considered one-dimensional owing to the symmetrical structure of the cylinder. As a result, the problem state may be represented by the space variable r and the instantaneous time variable t. Then, the governing field equations in one-dimensional cylindrical coordinates take the following forms

$$u_r = u(r, t),\ u_\phi(r, t) = u_z(r, t) = 0 \tag{21}$$

$$e_{rr} = \frac{\partial u}{\partial r},\ e_{\phi\phi} = \frac{u}{r} \tag{22}$$

$$\begin{aligned} \sigma_{rr} &= (2\mu + \lambda)\frac{\partial u}{\partial r} + \lambda\frac{u}{r} - \gamma\theta \\ \sigma_{\phi\phi} &= (2\mu + \lambda)\frac{u}{r} + \lambda\frac{\partial u}{\partial r} - \gamma\theta \end{aligned} \tag{23}$$

$$\frac{\partial \sigma_{rr}}{\partial r} + \frac{\sigma_{rr} - \sigma_{\phi\phi}}{r} = \rho\frac{\partial^2 u}{\partial t^2} \tag{24}$$

$$(\lambda + 2\mu)\frac{\partial}{\partial r}\left(\frac{\partial u}{\partial r} + \frac{u}{r}\right) - \gamma\frac{\partial \theta}{\partial r} = \rho\frac{\partial^2 u}{\partial t^2} \tag{25}$$

$$\begin{aligned} &\left(1 + \tau_q ABD_t^{(\alpha)}\right)\left(\rho C_E \tau_1^{\beta-1} ABD_t^{(\beta)}\theta + \gamma T_0 \tau_1^{\beta-1} ABD_t^{(\beta)}\left(\frac{\partial u}{\partial r} + \frac{u}{r}\right)\right) \\ &= K\left(1 + \tau_\theta ABD_t^{(\alpha)}\right)\nabla^2\theta \end{aligned} \tag{26}$$

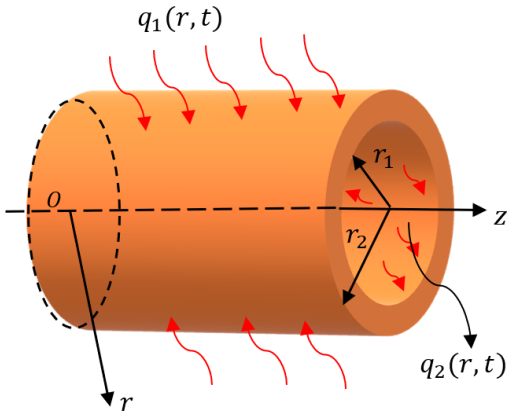

Figure 1. Isotropic traction-free hollow cylinder due to varying temperatures.

The following non-dimensional variables are introduced:

$$\begin{aligned} &\{r', u', r'_1, r'_2\} = c_0\eta\{r, u, r_1, r_2\}, \quad \{t, \tau'_q, \tau'_\theta, \tau'_1\} = c_0^2\eta\{t, \tau_q, \tau_\theta, \tau_1\}, \\ &\theta' = \frac{\theta}{T_0},\ \sigma'_{ij} = \frac{\sigma_{ij,}}{\mu},\ \eta = \frac{\rho C_E}{K},\ c_0 = \sqrt{\frac{\lambda+2\mu}{\rho}}. \end{aligned} \tag{27}$$

In the non-dimensional forms, the governing equations can be expressed as

$$a^2\frac{\partial}{\partial r}\left(\frac{\partial u}{\partial r} + \frac{u}{r}\right) - b\frac{\partial \theta}{\partial r} = a^2\frac{\partial^2 u}{\partial t^2} \tag{28}$$

$$\begin{aligned} &\left(1 + \tau_q ABD_t^{(\alpha)}\right)\left(\tau_1^{\beta-1} ABD_t^{(\beta)}\theta + g\tau_1^{\beta-1} ABD_t^{(\beta)}\left(\frac{\partial u}{\partial r} + \frac{u}{r}\right)\right) \\ &= \left(1 + \tau_\theta ABD_t^{(\alpha)}\right)\left(\frac{\partial^2 \theta}{\partial r^2} + \frac{1}{r}\frac{\partial \theta}{\partial r}\right) \end{aligned} \tag{29}$$

$$\begin{aligned}\sigma_{rr} &= a^2\frac{\partial u}{\partial r} + (a^2-2)\frac{u}{r} - b\theta \\ \sigma_{\phi\phi} &= a^2\frac{u}{r} + (a^2-2)\frac{\partial u}{\partial r} - b\theta\end{aligned} \tag{30}$$

where

$$a^2 = \frac{\lambda+2\mu}{\mu}, g = \frac{\gamma^2 T_0}{\rho^2 C_E c_0^2}, b = \frac{\gamma T_0}{\mu}. \tag{31}$$

The method of potential for a set of uncoupled linear partial differential equations using the potential approach is a common and simple procedure. It is often used in the fields of elasticity and thermoelasticity. When using this potential function, the equations of motion, as well as the thermal conductivity equation, are simplified into a single partial differential equation governing the potential function. Then, as in the next section, this partial differential equation is reduced to an ordinary differential equation by applying the integral Laplace transform method to suppress the time variable. After solving this ordinary differential equation, the studied physical fields such as displacement, temperature change, and thermal stresses in the Laplace field are calculated.

By inserting the displacement potential function $u = \frac{\partial \varphi}{\partial r}$ into Eqs (28)–(30), yields

$$a^2\left(\nabla^2 - \frac{\partial^2}{\partial t^2}\right)\varphi = b\theta \tag{32}$$

$$\begin{aligned}&\left(1+\tau_q ABD_t^{(\alpha)}\right)\left(\tau_1^{\beta-1} ABD_t^{(\beta)}\theta + g\tau_1^{\beta-1} ABD_t^{(\beta)}\nabla^2\varphi\right) \\ &= \left(1+\tau_\theta ABD_t^{(\alpha)}\right)\left(\frac{\partial^2\theta}{\partial r^2} + \frac{1}{r}\frac{\partial\theta}{\partial r}\right)\end{aligned} \tag{33}$$

$$\begin{aligned}\sigma_{rr} &= a^2\frac{\partial^2\varphi}{\partial r^2} + \frac{(a^2-2)}{r}\frac{\partial\varphi}{\partial r} - b\theta \\ \sigma_{\phi\phi} &= (a^2-2)\frac{\partial^2\varphi}{\partial r^2} + \frac{a^2}{r}\frac{\partial\varphi}{\partial r} - b\theta\end{aligned}. \tag{34}$$

5. Initial and boundary conditions

The following initial conditions are considered

$$u(r,0) = \frac{\partial u(r,0)}{\partial r} = 0,\ \theta(r,0) = \frac{\partial\theta(r,0)}{\partial r} = 0. \tag{35}$$

The following are the internal and external thermal boundary conditions for heat transfer and convection between the cylinder surfaces when $t > 0$ [52]:

$$\begin{aligned}q(r_1,t) &= h_1(f_1-\theta), \\ q(r_2,t) &= h_2(\theta-f_2),\end{aligned} \tag{36}$$

where h_1 and h_2 are constant coefficients of surface heat transfer of inner and outer surroundings, often known as a Biot number, and f_1 and f_2 inner and outer surrounding temperatures. In addition, it is assumed that the mechanical boundary conditions on the cylinder surfaces when $t > 0$ are free of traction i.e.

$$\begin{aligned} \sigma_{rr}(r_1, t) &= 0, \\ \sigma_{rr}(r_2, t) &= 0. \end{aligned} \tag{37}$$

6. Solution methodology

The Laplace transform is a technique used by many researchers. An ordinary differential equation may be transformed into an algebraic equation using the Laplace transform, which is often easier to work with. Another feature of the Laplace transform is that it may be used to deal with external forces that are either impulsive or off for a symmetric or asymmetric duration of time.

We can get the following result by applying the Laplace transform to both sides of the Eqs (32)–(34)

$$(\nabla^2 - s^2)\bar{\varphi} = \frac{b}{a^2}\bar{\theta} \tag{38}$$

$$g\omega\nabla^2\bar{\varphi} = (\nabla^2 - \omega)\bar{\theta} \tag{39}$$

$$\begin{aligned} \bar{\sigma}_{rr} &= \left(a^2 \frac{\mathrm{d}^2}{\mathrm{d}r^2} + (a^2 - 2)\frac{1}{r}\frac{\mathrm{d}}{\mathrm{d}r}\right)\bar{\varphi} - b\bar{\theta} \\ \bar{\sigma}_{\phi\phi} &= \left((a^2 - 2)\frac{\mathrm{d}^2}{\mathrm{d}r^2} + a^2 \frac{1}{r}\frac{\mathrm{d}}{\mathrm{d}r}\right)\bar{\varphi} - b\bar{\theta} \end{aligned} \tag{40}$$

where

$$\omega = \frac{\tau_1^{\beta-1} G(s,\beta)\left(1+\tau_q G(s,\alpha)\right)}{(1+\tau_\theta G(s,\alpha))},\ G(s,\alpha) = \frac{s^\alpha}{s^{\alpha(1-\alpha)+\alpha}},\ G(s,\beta) = \frac{s^\beta}{s^{\beta(1-\beta)+\beta}}. \tag{41}$$

We can get the following fourth order ordinary differential equation by removing $\bar{\theta}$ from Eqs (38) and (39)

$$\left(\frac{\mathrm{d}^2}{\mathrm{d}r^2} + \frac{1}{r}\frac{\mathrm{d}}{\mathrm{d}r} - \xi_1^2\right)\left(\frac{\mathrm{d}^2}{\mathrm{d}r^2} + \frac{1}{r}\frac{\mathrm{d}}{\mathrm{d}r} - \xi_2^2\right)\bar{\varphi} = 0. \tag{42}$$

The roots of the following equation are ξ_1^2 and ξ_2^2

$$\xi^4 - \left(\omega + \frac{g\omega b}{a^2} + s^2\right)\xi^2 + s^2\omega = 0. \tag{43}$$

The general solution of $\bar{\varphi}$ after solving the differential equation (36) can be determined as

$$\bar{\varphi} = A_1 I_0(\xi_1 r) + A_2 I_0(\xi_2 r) + B_1 K_0(\xi_1 r) + B_2 K_0(\xi_2 r). \tag{44}$$

In Eq (44), the well-known modified Bessel functions $I_0(z)$ and $K_0(z)$ are used. Also, from the boundary conditions (36) and (37), the integration constants A_i, B_i $(i = 1,2)$ can be determined.

When we plug Eq (44) into Eq (38), we get

$$\bar{\theta} = \frac{a^2}{b}\sum_{i=1}^{2}(\xi_i^2 - s^2)[A_i I_0(\xi_i r) + B_i K_0(\xi_i r)]. \tag{45}$$

The solution for $\bar{u}$ can be obtained after using Eq (44) as

$$\bar{u} = \frac{\mathrm{d}\bar{\varphi}}{\mathrm{d}r} = A_1\xi_1 I_1(\xi_1 r) + A_2\xi_2 I_1(\xi_2 r) - B_1\xi_1 K_1(\xi_1 r) - B_2\xi_1 K_1(\xi_2 r). \tag{46}$$

Using the solutions for $\bar{\varphi}$ and $\bar{\theta}$, then solutions to the thermal stresses can be determined as

$$\bar{\sigma}_{rr} = \sum_{i=1}^{2}\left\{A_i\left[a^2s^2 I_0(\xi_i r) - \frac{2\xi_i}{r} I_1(\xi_i r)\right] + B_i\left[a^2s^2 K_0(\xi_i r) + \frac{2\xi_i}{r} K_1(\xi_i r)\right]\right\} \tag{47}$$

$$\bar{\sigma}_{\phi\phi} = \sum_{i=1}^{2}\left\{A_i\left[(a^2s^2 - 2\xi_i^2) I_0(\xi_i r) + \frac{2\xi_i}{r} I_1(\xi_i r)\right]\right.$$

$$\left. + B_i\left[(a^2s^2 - 2\xi_i^2) K_0(\xi_i r) - \frac{2\xi_i}{r} K_1(\xi_i r)\right]\right\}. \tag{48}$$

By using the non-dimensional figures (27) of the modified Fourier law of thermal conductivity (9) with the Atangana-Baleanu time-fractional derivative, then we have

$$\left(1 + \tau_q ABD_t^{(\alpha)}\right) q_r = -\left(1 + \tau_\theta ABD_t^{(\alpha)}\right)\frac{\mathrm{d}\theta}{\mathrm{d}r}. \tag{49}$$

Then the non-dimensional boundary conditions (30) and (31) in the Laplace transform domain have the forms

$$\left(1 + \tau_\theta ABD_t^{(\alpha)}\right)\frac{\mathrm{d}\theta}{\mathrm{d}r} = h_1\left(1 + \tau_q ABD_t^{(\alpha)}\right)(\theta - f_1), \text{at } r = r_1 \tag{50}$$

$$\left(1 + \tau_\theta ABD_t^{(\alpha)}\right)\frac{\mathrm{d}\theta}{\mathrm{d}r} = h_2\left(1 + \tau_q ABD_t^{(\alpha)}\right)(f_2 - \theta), \text{at } r = r_2. \tag{51}$$

After applying the Laplace transform to the boundary conditions (50) and (51), we arrive at the following

$$\left(\frac{\mathrm{d}}{\mathrm{d}r} - \psi_1\right)\bar{\theta} = -\frac{\psi_1 f_1}{\mathrm{s}}, \text{at } r = r_1, \tag{52}$$

$$\left(\frac{\mathrm{d}}{\mathrm{d}r} + \psi_2\right)\bar{\theta} = \frac{\psi_2 f_2}{\mathrm{s}}, \text{at } r = r_2, \tag{53}$$

where

$$\psi_1 = \frac{h_1\left(1+\tau_q G(s,\alpha)\right)}{\left(1+\tau_\theta G(s,\alpha)\right)},\ \psi_2 = \frac{h_2\left(1+\tau_q G(s,\alpha)\right)}{\left(1+\tau_\theta G(s,\alpha)\right)}. \tag{54}$$

In addition, the boundary conditions (37) in the domain of the Laplace transform take the form

$$\begin{aligned}\bar{\sigma}_{rr}(r_1, s) &= 0,\\ \bar{\sigma}_{rr}(r_2, s) &= 0.\end{aligned} \tag{55}$$

When we apply the thermal boundary conditions (52) to Eqs (55), we can obtain the following linear system of equations:

$$\sum_{i=1}^{2}\xi_i(\xi_i^2 - s^2)(\xi_i - \psi_1)[A_i I_1(\xi_i r_1) - B_i K_1(\xi_i r_1)] = -\frac{b\psi_1 f_1}{sa^2}, \tag{56}$$

$$\sum_{i=1}^{2} \xi_i(\xi_i^2 - s^2)(\xi_i + \psi_2)[A_i I_1(\xi_i r_2) - B_i K_1(\xi_i r_2)] = \frac{b\psi_2 f_2}{sa^2}, \tag{57}$$

$$\sum_{i=1}^{2} \left\{ A_i \left[a^2 s^2 I_0(\xi_i r_1) - \frac{2\xi_i}{r_1} I_1(\xi_i r_1) \right] + B_i \left[a^2 s^2 K_0(\xi_i r_1) + \frac{2\xi_i}{r_1} K_1(\xi_i r_1) \right] \right\} = 0 \tag{58}$$

$$\sum_{i=1}^{2} \left\{ A_i \left[a^2 s^2 I_0(\xi_i r_2) - \frac{2\xi_i}{r_2} I_1(\xi_i r_2) \right] + B_i \left[a^2 s^2 K_0(\xi_i r_2) + \frac{2\xi_i}{r} K_1(\xi_i r_2) \right] \right\} = 0. \tag{59}$$

The four constants $A_i, B_i,\ (i = 1,2)$ may be calculated by solving the system equations (65)–(59).

7. Numerical calculation and discussion

Before the discussions, it is necessary to first calculate the numerical values of the different physical fields in the space-time field. Due to the difficulty of obtaining the inverse Laplace transforms of the studied functions, we will use one of the most accurate and effective methods that are frequently used in the field of thermoelasticity. To get the Laplace inversion transform, the Riemann-sum approximation approach is utilized [53]. Any function in the Laplace domain may be inverted to the time domain using this approach by applying the formula below:

$$h(r,t) = \frac{e^{\varsigma t}}{t}\left(\frac{1}{2}\bar{h}(r,\varsigma) + Re\sum_{n=1}^{N} \bar{h}\left(r, \varsigma + \frac{in\pi}{t}\right)(-1)^n\right). \tag{60}$$

According to several numerical experiments, $\varsigma \cong 4.7$ is a good choice for quick convergence [49]. The Mathematica programming language was used to create numerical calculations.

In this section, we will look at how the two-time fractional orders α and β affect the response of thermoelastic materials. For computational and comparative purposes, we consider a numerical example. The copper material's physical constants are employed [54]

$$\{\lambda, \mu\} = \{7.76, 3.86\} \times 10^{10}\text{kgm}^{-1}\text{s}^{-2}, \qquad \rho = 8954\ \text{kg/m}^3,$$
$$K = 386\ \text{W/(mK)}, C_E = 3.381\ \text{Jkg/K}, \varepsilon = 0.0168.$$

The following functions f_1 and f_2 can also be used for purposes of illustration [44]

$$f_1(r,t) = 1.5 + 0.5\cos(13t), f_2(r,t) = 1.0.$$

The numerical results of the investigated fields along the radial distance r are provided for various values of the fractional-order parameters α and β as well as for the instance of time t. The numerical calculation was performed using the **MATHEMATICA** programming language. The profiles for temperature θ and displacement u, as well as the thermal stresses σ_{rr} and $\sigma_{\phi\phi}$ are obtained separately in Tables 1–4 and Figures 2–9 using the numerical approach described in [53] when the nondimensional radii are $r_1 = 1$ and $r_2 = 3$.

7.1. Effect of time-fractional order parameters

Frequently found in diverse applications in fluid mechanics, viscoelasticity, physics, structural mechanics, biology, systems theory, and design, fractional-order PDEs have been an important topic of many investigations. The non-local quality of the fractional-order differential equations is the most

important feature to be used in this and other applications. Fractional calculus has been effectively used in the study of thermoelasticity for the last several years. In the present scenario, the effects of fractional order parameters α and β on the thermoelastic studied fields were examined.

As mentioned in Section 3, several thermoelastic models with and without fractional orders presented in this category can be used as special cases for the new proposed fractional thermoelastic model with fractional order parameters α and β (**2FMTE**). These models depend on the order of fractional calculus and are:

• The fractional thermoelastic model (**1FABTE**) with the Atangana-Baleanu (AB) fractional operator [34] and single fractional order ($\beta = 1$).

• The thermoelastic fractional model (**FSCTE**) with the Caputo fractional derivative [23] and single fractional order ($\beta = 1$) proposed by Sherief [24].

• The dual-phase lag fractional thermoelastic model (**FEDPL**) with one fractional order ($\beta = 1$) proposed by Ezzat et al. [43].

• The two-phase delayed thermoelastic model (**DPL**) [8], the Lord-Shulman thermoelastic model (**LS**) [3] and classical thermoelasticity theory (**CTE**).

A comparison of several models of thermoelasticity will be presented to confirm the results. To illustrate the comparisons between the various fractional thermoelastic models, it is useful to organize the numerical results into figures and tables. In addition, the data obtained will be presented in tabular form to help other scientists compare and verify the results. For different distances r, $(1 \leq r \leq 3)$ within the solid cylinder, the numerical results are presented in Tables 1–4 for several thermoelastic models with and without fractional orders. The differences between different thermoelastic models with fractional operators only are also shown in Figures 2–5. Although the values differ between the models, there are commonalities in the behavior of the distributions, as shown in Tables 1–4 and Figures 2–5.

Table 1 shows the temperature fluctuations as a function of distance x and time t for various fractional differentiation α and β values. Table 1 shows that the fractional differentiation parameters α and β have a significant impact on the temperature change. By referring to the table, we can see that there is a variance in the temperature profile values for all thermoelastic formulations with and without fractional orders. We also note from the table that the temperature values vary more in the case of thermoelastic models without a fractional differential than in the case of other models of thermoelasticity with fractional differential operators. It is clear that raising the values of the fractional-order modulus raises the temperature value. In other words, the presence of fractional operators reduces the propagation of the heat wave within the medium. For this reason, one of the reasons that partial calculus is gaining popularity is that it is more realistic and compatible with physical phenomena.

Figure 2 shows the temperature distributions for fractional thermoelastic models in the r-direction of the hollow cylinder (**FSCTE**, **FEDPL**, **1FABTE**, and **2FABTE**). One important observation that can be deduced from Figure 1 is that the temperature distribution curves in the case of thermoelastic models that include the Atangana-Baleanu fractional operator (**1FABTE** and **2FABTE**) are lower than in the case of thermoelastic models that include the fractional Caputo derivative (**FSCTE** and **FEDPL**). For fractional thermoelastic theories, wave propagation with limited speeds is exhibited in all curves.

Table 1. The temperature distribution θ under several thermoelastic models with and without fractional derivatives.

r	CTE	LS	DPL	FSCTE	FEDPL	1FABTE	2FABTE
1.0	0.2722770	0.1989800	0.2371690	0.1527580	0.1877100	0.1713860	0.1271580
1.2	0.1133480	0.0635338	0.0884457	0.0374171	0.0568620	0.0471606	0.0249330
1.4	0.0505113	0.0212545	0.0348813	0.0095773	0.0180318	0.0135972	0.0051213
1.6	0.0261163	0.00776461	0.0154342	0.0025526	0.00611499	0.0041346	0.0010821
1.8	0.0200238	0.00394068	0.0102354	0.0008982	0.00296159	0.0017385	0.0002803
2.0	0.0260408	0.00558839	0.0135809	0.0010329	0.00373252	0.0021143	0.0002805
2.2	0.0465928	0.0117216	0.0267181	0.0030551	0.00903844	0.0055644	0.0010032
2.4	0.0973929	0.0323722	0.0580565	0.0097637	0.02433430	0.0164482	0.0042860
2.6	0.2207760	0.0865866	0.1400750	0.0381335	0.06703500	0.0498439	0.0176783
2.8	0.4860630	0.1902680	0.3611190	0.1040010	0.21520400	0.1756950	0.0835381
3.0	0.9436060	0.6716030	0.7967400	0.4768660	0.59308400	0.5241260	0.3590820

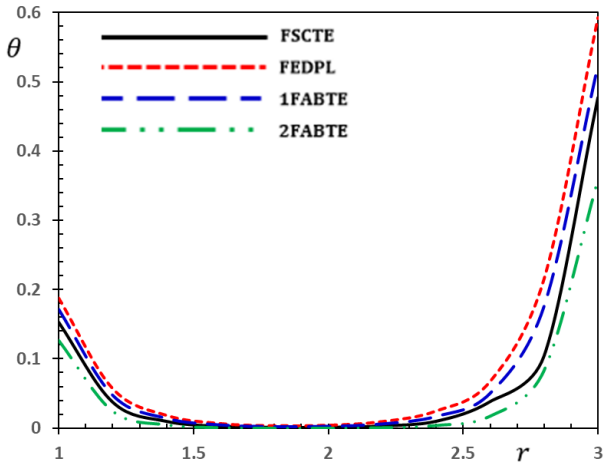

Figure 2. The temperature distribution θ under different fractional thermoelastic models.

Table 2 shows how the displacement $u(r,t)$ varies across the cylinder radius for different values of the fractional-order parameters α and β. From the table, we can see that the fractional-order coefficients have significant effects on the displacement values. The displacement begins with negative values on the inner surface of the cylinder, which is influenced by the time-dependent heat flow and progressively increases to values close to zero on the outer surface of the cylinder, which is impacted by a constant heat flow. The concept of combined thermal elasticity (**CTE**) is based on a system of parabolic equations, which accurately predicts an infinite velocity of heat diffusion, while generalized thermal conductivity models (with and without partial derivatives) (**LS**, **DPL**, **FSCTE**, **FEDPL**, **1FABTE**, and **2FABTE**) are based on hyperbolic governing equations, which recognize the bounded velocity of heat and mechanical signals. As can be seen from the table, the displacement changes drastically when the fractional differential orders differ. The fractional-order parameters have been shown to be exactly related to the radial displacement $u(r,t)$. More precisely, the result shows that the absolute value of the dynamic displacement is inversely proportional to the fractional orders.

Table 2. The displacement distribution u under several thermoelastic models with and without fractional derivatives.

r	CTE	LS	DPL	FSCTE	FEDPL	1FABTE	2FABTE
1.0	-0.22798500	-0.06352840	-0.14471200	-0.0447889	-0.0929007	-0.0674292	-0.0352852
1.2	-0.01033190	-0.00287213	-0.00655342	-0.0020242	-0.0042040	-0.0030499	-0.0015918
1.4	-0.00046746	-0.000127262	-0.000294953	-9.131E-05	-0.0001893	-0.0001374	-7.037E-05
1.6	-1.88682E-05	-4.34725E-06	-1.14134E-05	-3.855E-06	-7.542E-06	-5.631E-06	-2.527E-06
1.8	-1.15714E-06	-3.76784E-08	-4.7781E-07	-1.21E-07	-1.872E-07	-1.467E-07	-3.127E-09
2.0	-3.32335E-06	-8.83852E-07	-1.94194E-06	-9.094E-08	-6.116E-07	-2.604E-07	-2.458E-07
2.2	-8.10738E-06	-2.95603E-06	-5.32627E-06	-4.391E-07	-2.108E-06	-1.052E-06	-1.017E-06
2.4	-1.72836E-05	-7.66960E-06	-1.25643E-05	-1.869E-06	-6.179E-06	-3.635E-06	-3.57E-06
2.6	-3.45915E-05	-2.05792E-05	-2.75809E-05	-7.385E-06	-1.682E-05	-1.168E-05	-1.15E-05
2.8	-4.13714E-05	-3.09996E-05	-3.72666E-05	-1.835E-05	-2.894E-05	-2.370E-05	-2.41E-05
3.0	0.005430100	0.000324307	0.000430503	0.0001713	0.0002952	0.0002290	0.0002198

Figure 3 depicts the displacement $u(r,t)$ profile along the r-axis for several fractional thermoelastic models (**FSCTE**, **FEDPL**, **1FABTE**, and **2FABTE**). It is also worth noting that for various values of the fractional-order parameters, the highest points of the displacement curves occur at the inner surface of the hollow cylinder. We can see from the graph that the difference is large at the inner surface of the hollow cylinder, and that as r increases, the difference becomes less noticeable until we reach $1.4 \leq r \leq 3$. The curves of the different theories are similar in their behavior but significantly different in magnitude. The displacement curves for thermoelastic models using the Atangana-Baleanu fractional operator (**1FABTE** and **2FABTE**) are lower than for thermoelastic models incorporating the fractional Caputo derivative (**FSCTE** and **FEDPL**).

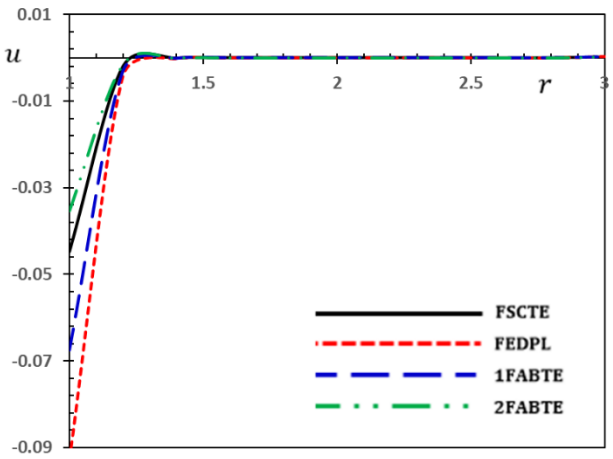

Figure 3. The displacement distribution u under different fractional thermoelastic models.

Table 3 shows how the thermal stress σ_{rr} varies across the cylinder radius for different values of the fractional-order parameters α and β. Also, Figure 3 depicts the stress σ_{rr} profile along the r-axis for several fractional thermoelastic models (**FSCTE**, **FEDPL**, **1FABTE**, and **2FABTE**). It is observed that the radial stress σ_{rr} fulfills the boundary criteria. At cylindrical boundary surfaces free

of traction, the radial stress is zero. In all thermoelasticity models, the difference is small in the range $1.8 \leq r \leq 2.1$ and large in the region $2.1 \leq r \leq 3$. For $1 \leq r \leq 1.8$, all models then approach zero. It is clear that the stress σ_{rr} values are reduced when the values of the fractional-order parameters α and β are reduced. Figure 4 demonstrates how the amplitude of the stress σ_{rr} progressively grows from the inner surface to the outer surface, and then rapidly declines to zero. The compressive radial stress is also shown along the outer cylindrical surface. There is a distinct difference in the radial stress σ_{rr} values across the fractional-order models, and the magnitude of thermal stress in the proposed models (**1FABTE** and **2FABTE**) is lower than in the previous **FSCTE** and **FEDPL** models.

Table 3. The radial stress σ_{rr} under several thermoelastic models with and without fractional derivatives.

r	CTE	LS	DPL	FSCTE	FEDPL	1FABTE	2FABTE
1.0	0	0	0	0	0	0	0
1.2	-0.000491946	-0.000042632	-0.000174283	-3.15E-06	-2.23521E-05	-9.712E-06	-3.985E-07
1.4	-0.00116129	-0.000100246	-0.00044089	-1.106E-05	-6.67452E-05	-3.116E-05	-1.718E-06
1.6	-0.00241987	-0.000323302	-0.00100674	-3.8E-05	-0.000185414	-9.411E-05	-7.201E-06
1.8	-0.00492269	-0.000731596	-0.00229513	-0.0001273	-0.000515789	-0.0002846	-3.038E-05
2.0	-0.00989298	-0.00223525	-0.00525188	-0.0004394	-0.00145152	-0.000869	-0.0001288
2.2	-0.0200995	-0.00541043	-0.0118231	-0.0015276	-0.00408627	-0.0026768	-0.0005486
2.4	-0.0431250	-0.0151136	-0.0263601	-0.0049693	-0.0111864	-0.0080473	-0.002344
2.6	-0.0969068	-0.0399912	-0.0627439	-0.0186561	-0.0312626	-0.0238614	-0.0093514
2.8	-0.1941170	-0.0742848	-0.1446800	-0.0415447	-0.0876719	-0.0718103	-0.0352842
3.0	0	0	0	0	0	0	0

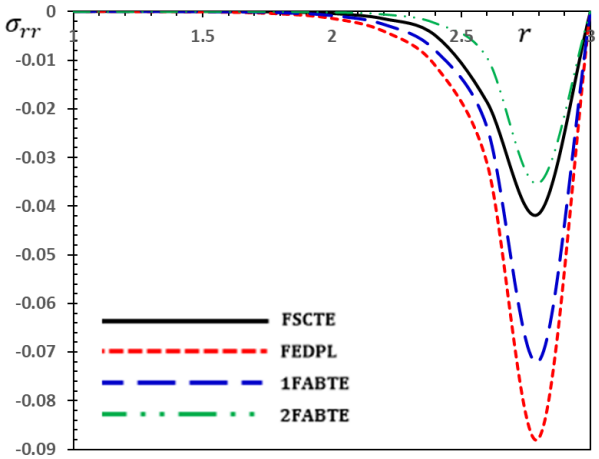

Figure 4. The radial stress σ_{rr} under different fractional thermoelastic models.

The influence of fractional order parameters α and β on the hoop stress $\sigma_{\phi\phi}$ patterns versus distance r is presented in Table 4. Figure 5 also shows the hoop stress $\sigma_{\phi\phi}$ for various fractional thermoelastic models. The numerical findings for $\sigma_{\phi\phi}$ show that the behavior of hoop stress $\sigma_{\phi\phi}$ is similar to that of thermal stress σ_{rr}, although it differs only at the beginning point at $r = 3$. The stress curves for coupled thermoelastic models have been discovered to be greater than those for LS and DPL

thermoelasticity models. We discovered that the fractional-order parameters α and β have a considerable impact on the hoop stress field distribution. As the values of the fractional parameters increase, the values of all thermal fields σ_{rr} and $\sigma_{\phi\phi}$ decrease, and the wave propagation velocity decreases more rapidly.

Table 4. The hoop stress $\sigma_{\phi\phi}$ under several thermoelastic models with and without fractional derivatives.

r	CTE	LS	DPL	FSCTE	FEDPL	1FABTE	2FABTE
1.0	-0.0896945	-0.000033926	-0.000183945	-1.964E-06	-1.796E-05	-7.014E-06	-1.921E-07
1.2	-0.091114	-5.02423E-05	-0.000226824	-3.34E-06	-2.588E-05	-1.081E-05	-3.911E-07
1.4	-0.0958447	-9.82654E-05	-0.000446397	-1.034E-05	-6.467E-05	-2.973E-05	-1.547E-06
1.6	-0.103518	-0.000309999	-0.000981334	-3.518E-05	-0.0001762	-8.85E-05	-6.441E-06
1.8	-0.114255	-0.000696467	-0.00222267	-0.0001175	-0.0004887	-0.0002669	-2.711E-05
2.0	-0.128295	-0.00213372	-0.00507718	-0.000405	-0.0013738	-0.0008139	-0.0001147
2.2	-0.146094	-0.00514363	-0.011413	-0.0014086	-0.0038636	-0.0025056	-0.0004885
2.4	-0.168354	-0.0144146	-0.0254315	-0.0045728	-0.0105656	-0.007527	-0.0020932
2.6	-0.195295	-0.0383648	-0.0610044	-0.0174499	-0.0298176	-0.022541	-0.0084657
2.8	-0.225621	-0.0773127	-0.148348	-0.0428086	-0.0893514	-0.072986	-0.0353343
3.0	-0.312362	-0.137042	-0.162114	-0.0974108	-0.119282	-0.106807	-0.0732922

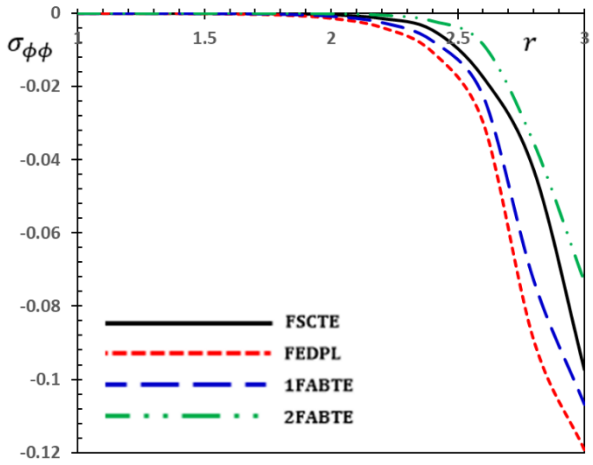

Figure 5. The hoop stress $\sigma_{\phi\phi}$ under different fractional thermoelastic models.

It is clear from Figure 4 that, for small-time values, the pressures are of a compressive nature. Also, the solution is located in a limited region of space surrounding the heating source, and there is zero outside of this region. This is because the solution found using generalized fractional differential equations of thermoelasticity exhibits patterns of wave propagation and behavior at finite rates. It is noted that the solution is limited to a limited region of space surrounding the inner surface of the cylinder for small values of time and zero outside this region. These results differ from the twofold

theory, in which you would expect the heat wave to cover the entire cylinder at the same instant. As a result, for any short period of time, although the solution is very small, it is not identical to zero.

The findings of this study provide the concept of generalized thermoelasticity in fractional order as a novel innovation and development in the field of thermoelasticity subjected to time-dependent heat supplies. According to this idea, we can create a new classification of all materials based on their fractional parameters, which will serve as a new indicator of their capacity to conduct thermal energy. Despite the good results obtained through the new proposed model, it can be said theoretically that no model of thermal elasticity with fractional order can be more accurate than other models unless it is experimentally tested.

7.2. Effects of time instant

In this scenario, we will investigate the influence of instantaneous time t on the behavior of several physical distributions. In this case, we will consider the new model that contains fractional derivatives with two fractional-orders α and β (**2FABTE**). To understand the topic of the effect of the time t change on the studied physical responses in more depth, we will present a set of figures (see Figures 6–9). When the fractional-order parameters α and β are held constant, the change will occur concurrently with the radius r, $(1 \leq r \leq 3)$ and also over time t, $(0.05 \leq t \leq 0.12)$.

Figures 6–9 show that temperature change θ, radial and hoop stress fields σ_{rr} and $\sigma_{\phi\phi}$, and radial displacement u distribution are particularly sensitive to instantaneous changes in time t. It was also discovered that instantaneous time t has a significant impact on the behavior of the studied physical fields.

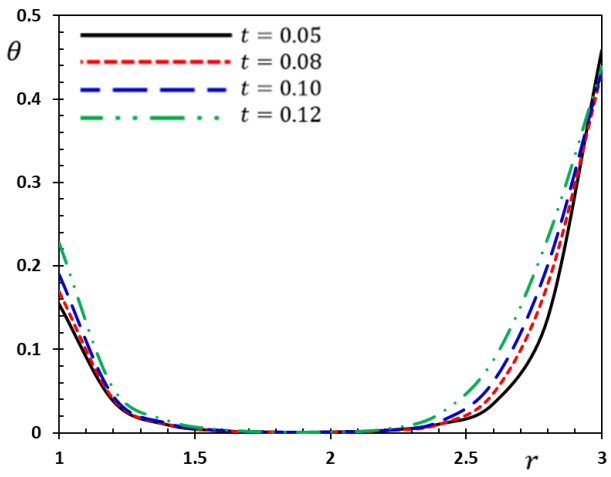

Figure 6. The temperature variation θ for different instant time t values.

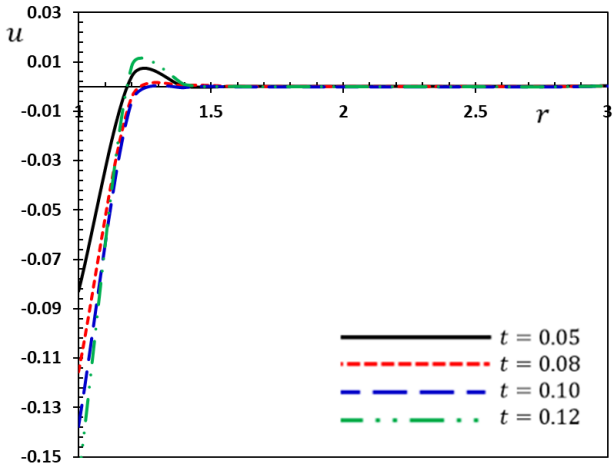

Figure 7. The variation of displacement U for different instant time t values.

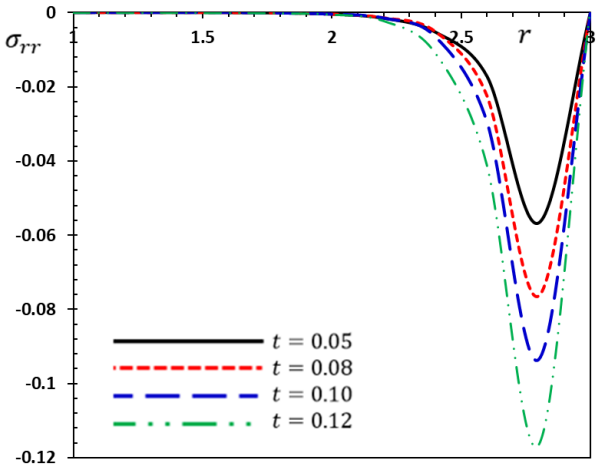

Figure 8. The variation of the radial stress σ_{rr} for different instant time t values.

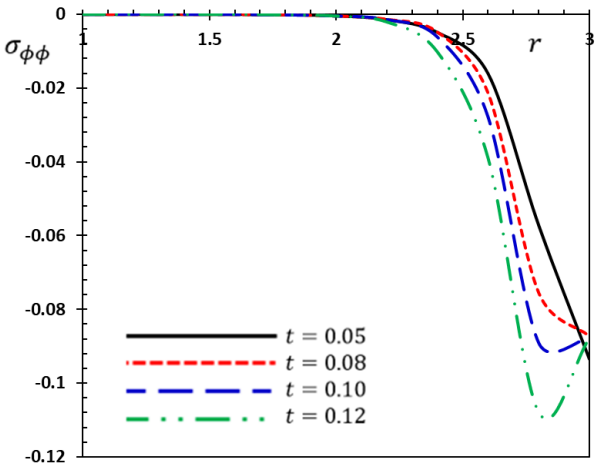

Figure 9. The distribution of the hoop stress $\sigma_{\phi\phi}$ for different instant time t values.

Figure 6 depicts the influence of time t on the temperature θ profile. Figure 6 depicts how the temperature difference at any given distance r rises with time t. This leads to a lengthening of the wavelength and higher energy of the thermal dispersion wave. Figure 7 depicts the influence of time t on the graph of the displacement function $u(r,t)$. Figure 6 shows that the displacement u is highly dependent on the time t value. As the value of time t grows, so does the absolute value of displacement u. Figure 9 shows that the radial stress σ_{rr} satisfies the stress-free conditions at $r = r_1$ and $r = r_2$ and has a possible characteristic behavior. Figures 8 and 9 also show that the instant time t increases the absolute value of the radial and hoop stresses σ_{rr} and $\sigma_{\phi\phi}$.

Thermal stress σ_{rr} is a dynamic process. This means that the expanding area gradually creeps into the neighboring area over time and then gets bigger and bigger. As a result, the curve and the magnitude of the radial stress σ_{rr} behavior increase. Also, due to the wave effect of finite heat, the non-zero region of the radial stress σ_{rr} at any time is also limited. This means that, over time, heat flows into the deeper layers of the medium at a limited rate. The thermal turbulent area and radial stress increase in proportion to the studied moment.

8. Conclusions

The present article presents a modified model of thermal conductivity with two fractional orders and two-phase delays. The proposed model is based on the concept of a fractional integrated Atangana-Baleanu (AB) operator with non-singular and non-localized kernels. This model was applied to examine the vibrations of thermoelastic in a traction-free annular cylinder subjected to a time-dependent variable temperature. Some numerical values are presented in tables and figures to analyze the effects of fractional indicators on all physical field variables. The analytic solutions of the governing equations in the Laplace domain, which are then inverted in the time domain, are derived using the Honig and Hirdes technique. To study the effects of fractional orders and the properties of instantaneous time, some comparisons between different thermoelastic models in the presence and absence of fractional differential operators with fractional orders were tabulated and presented graphically. The following are the main results obtained from the discussions:

• The values of all investigated physical variables are greatly influenced by the fractional-order parameters that have been suggested in the heat conduction model with fractional operators.

• The modified thermoelastic model with fractional parameters and phase delays allows thermal and mechanical waves to propagate at limited speeds.

• The temperature distribution curves in the case of thermoelastic models that include the Atangana-Baleanu fractional operator (1FABTE and 2FABTE) are lower than in the case of thermoelastic models that include the fractional Caputo derivative (FSCTE and FEDPL).

• The presence of fractional operators reduces the propagation of the heat wave within the medium. According to this idea, we can create a new classification of all materials based on their fractional parameters, which will serve as a new indicator of their capacity to conduct thermal energy.

• Instantaneous time has a significant impact on the behavior of the studied physical fields.

• In future work, the improved governing equation for thermal conductivity with phase-delay times and including the integrated fractional Atangana-Baleanu operator can be extended to simulate real-world problems in many areas, including computational fluid dynamics, high-density polyethylene, and viscoelasticity. Also, in the biological sciences, physical sciences, and dipolar materials and engineering fields.

Nomenclature

λ, μ	Lamе́'s constants	K	thermal conductivity
α_t	coefficient of thermal expansion	∇^2	Laplacian operator
$\gamma = (3\lambda + 2\mu)\alpha_t$	coupling coefficient	t	instant time
T_0	reference temperature	ρ	material density
$\theta = T - T_0$	temperature increment	u_i	displacements
T	absolute temperature	F_i	body force vector
C_E	specific heat	Q	heat source
σ_{ij}	stress tensor	τ_θ, τ_q	phase − lag times
$e = u_{k,k}$	dilatation	α, β	fractional orders
e_{ij}	strain tensor	δ_{ij}	Kronecker function
r_1	inner radius	r_2	outer radius
f_1, f_2	inner and outer surrounding temperatures	r, ϕ, z	Cylindrical coordinate system
h_1, h_2	dimensionless heat transfer	∇	Hamilton operator

Acknowledgments

The authors extend their appreciation to the Deanship of Scientific Research at Jouf University for funding this work through research grant No. (DSR-2021-03-0380). We would also like to extend our sincere thanks to the College of Science and Arts in Al-Qurayyat for its technical support.

Conflict of interest

The authors declare no conflicts of interest.

References

1. Y. Povstenko, *Fractional thermoelasticity*, New York: Springer 2015.
2. Y. Povstenko, Theories of thermal stresses based on space-time-fractional telegraph equations, *Comput. Math. Appl.*, **64** (2012), 3321–3328. https://doi.org/10.1016/j.camwa.2012.01.066
3. H. W. Lord, Y. Shulman, A generalized dynamical theory of thermoelasticity, *J. Mech. Phys. Solids*, **15** (1967), 299–309. https://doi.org/10.1016/0022-5096(67)90024-5
4. A. E. Green, K. A. Lindsay, Thermoelasticity, *J. Elast*icity, **2** (1972), 1–7. https://doi.org/10.1007/BF00045689
5. A. E. Green, P. M. Naghdi, A re-examination of the basic postulates of thermomechanics, *Proc. R. Soc. A, Math. Phys. Eng. Sci.*, **432** (1991), 171–194. https://doi.org/10.1098/rspa.1991.0012
6. A. E. Green, P. M. Naghdi, On undamped heat waves in an elastic solid, *J. Therm. Stresses*, **15** (1992), 253–264. https://doi.org/10.1080/01495739208946136
7. A. E. Green, P. M. Naghdi, Thermoelasticity without energy dissipation, *J. Elast*icity, **31** (1993), 189–208. https://doi.org/10.1007/BF00044969
8. D. Y. Tzou, A unified field approach for heat conduction from macro- to micro-scales, *J. Heat Transfer*, **117** (1995), 8–16. https://doi.org/10.1115/1.2822329
9. D. S. Chandrasekharaiah, Hyperbolic thermoelasticity: A review of recent literature, *Appl. Mech. Rev.*, **51** (1998), 705–729. https://doi.org/10.1115/1.3098984

10. R. B. Hetnarski, J. Ignaczak, Generalized thermoelasticity, *J. Therm. Stres*ses, **22** (1999), 451–476. https://doi.org/10.1080/014957399280832
11. A. E. Abouelregal, Two-temperature thermoelastic model without energy dissipation including higher order time-derivatives and two phase-lags, *Mater. Res. Express*, **6** (2019), 116535. https://doi.org/10.1088/2053-1591/ab447f
12. A. E. Abouelregal, A novel generalized thermoelasticity with higher-order time-derivatives and three-phase lags, *Multidiscip. Model. Ma.*, **16** (2020), 689–711.
13. A. E. Abouelregal, Three-phase-lag thermoelastic heat conduction model with higher-order time-fractional derivatives, *Indian J. Phys.*, **94** (2020), 1949–1963. https://doi.org/10.1007/s12648-019-01635-z
14. H. Zhou, P. Li, Nonlocal dual-phase-lagging thermoelastic damping in rectangular and circular micro/nanoplate resonators, *Appl. Math. Model.*, **95** (2021), 667–687. https://doi.org/10.1016/j.apm.2021.02.035
15. H. Zhou, P. Li, Y. Fang, Single-phase-lag thermoelastic damping models for rectangular cross-sectional micro- and nano-ring resonators, *Int. J. Mech. Sci.*, **163** (2019), 105132. https://doi.org/10.1016/j.ijmecsci.2019.105132
16. H. Zhou, P. Li, W. Zuo, Y. Fang, Dual-phase-lag thermoelastic damping models for micro/nanobeam resonators, *Appl. Math. Model.*, **79** (2020), 31–51. https://doi.org/10.1016/j.apm.2019.11.027
17. H. Zhou, P. Li, Dual-phase-lagging thermoelastic damping and frequency shift of micro/nano-ring resonators with rectangular cross-section, *Thin-Wall. Struct.*, **159** (2021), 107309. https://doi.org/10.1016/j.tws.2020.107309
18. S. Deswal, K. K. Kalkal, R. Yadav, Response of fractional ordered micropolar thermoviscoelastic half-space with diffusion due to ramp type mechanical load, *Appl. Math. Model*., **49** (2017), 144–161. https://doi.org/10.1016/j.apm.2017.04.040
19. S. Mesloub, F. Aldosari, On a two-dimensional fractional thermoelastic system with nonlocal constraints describing a fractional Kirchhoff plate, *Adv. Differ. Equ*., **2021** (2021), 24. https://doi.org/10.1186/s13662-020-03188-6
20. B. Ross, The development of fractional calculus 1695–1900, *Hist. Math*., **4** (1977) 75–89. https://doi.org/10.1016/0315-0860(77)90039-8
21. K. S. Miller B. Ross, *An introduction to the fractional calculus and fractional differential equations*, John Wiley and Sons, New York, USA, 1993.
22. I. Podlubny, *Fractional differential equations*, New York, USA: Academic Press, 1999.
23. Y. Z. Povstenko, Fractional radial heat conduction in an infinite medium with a cylindrical cavity and associated thermal stresses, *Mech. Res. Commun*., **37** (2010), 436–440. https://doi.org/10.1016/j.mechrescom.2010.04.006
24. M. Caputo, Linear models of dissipation whose Q is almost frequency independent-II, *Geophys. J. Int.*, **13** (1967), 529–539. https://doi.org/10.1111/j.1365-246X.1967.tb02303.x
25. H. H. Sherief, A. M. A. El-Sayed, A. M. Abd El-Latief, Fractional order theory of thermoelasticity, *Int. J. Solids Struct*., **47** (2010), 269–275. https://doi.org/10.1016/j.ijsolstr.2009.09.034
26. M. A. Ezzat, Thermoelectric MHD non-Newtonian fluid with fractional derivative heat transfer, *Phys. B*, **405** (2010), 4188–4194. http://dx.doi.org/10.1016/j.physb.2010.07.009

27. A. S. El-Karamany, M. A. Ezzat, Convolutional variational principle, reciprocal and uniqueness theorems in linear fractional two-temperature thermoelasticity, *J. Therm. Stresses*, **34** (2011), 264–284. https://doi.org/10.1080/01495739.2010.545741
28. F. Hamza, M. Abdou, A. M. Abd El-Latief, Generalized fractional thermoelasticity associated with two relaxation times, *J. Therm. Stresses*, **37** (2014), 1080–1098. https://doi.org/10.1080/01495739.2014.936196
29. H. M. Youssef, Theory of fractional order generalized thermoelasticity. *J. Heat Transfer*, **132** (2010), 61301. https://doi.org/10.1115/1.4000705
30. Y. Z. Povstenko, Fractional heat conduction equation and associated thermal stress, *J. Therm. Stresses*, **28** (2004), 83–102. https://doi.org/10.1080/014957390523741
31. A. E. Abouelregal, A modified law of heat conduction of thermoelasticity with fractional derivative and relaxation time, *J. Mol. Eng. Mater.*, **8** (2020), 2050003. https://doi.org/10.1142/S2251237320500033
32. K. Zakaria, M. A. Sirwah, A. E. Abouelregal, A. F. Rashid, Photo-thermoelastic model with time-fractional of higher order and phase lags for a semiconductor rotating materials, *Silicon*, **13** (2021), 573–585. https://doi.org/10.1007/s12633-020-00451-z
33. A. E. Abouelregal, Modified fractional thermoelasticity model with multi-relaxation times of higher order: Application to spherical cavity exposed to a harmonic varying heat*, Waves Random Complex*, **31** (2021), 812–832. https://doi.org/10.1080/17455030.2019.1628320
34. A. E. Abouelregal, Fractional heat conduction equation for an infinitely generalized, thermoelastic, long solid cylinder, *Int. J. Comput. Methods Eng. Sci. Mech.*, **17** (2016), 374–381. https://doi.org/10.1080/15502287.2012.698700
35. M. Caputo, M. Fabrizio, A new definition of fractional derivative without singular kernel, *Prog. Fract. Differ. Appl.*, **1** (2015), 73–85.
36. A. Atangana, D. Baleanu, Caputo-Fabrizio derivative applied to groundwater flow within a confined aquifer, *J. Eng. Mech.*, **143** (2016), 1–16. https://doi.org/10.1061/(ASCE)EM.1943-7889.0001091
37. A. Atangana, D. Baleanu, New fractional derivatives with nonlocal and non-singular kernel: Theory and application to heat transfer model, *Therm. Sci*., 20 (2016), 763–769. https://doi.org/10.2298/TSCI160111018A
38. A. Atangana, J. F. Gómez-Aguilar, Decolonisation of fractional calculus rules: Breaking commutativity and associativity to capture more natural phenomena, *Eur. Phys. J. Plus*, **133** (2018), 1–22. https://doi.org/10.1140/epjp/i2018-12021-3
39. A. Atangana, I. Koca, Chaos in a simple nonlinear system with Atangana-Baleanu derivatives with fractional order, *Chaos Solit. Fract.*, **89** (2016), 447–454. https://doi.org/10.1016/j.chaos.2016.02.012
40. E. Uçar, S. Uçar, F. Evirgen, N. Özdemir, A fractional SAIDR model in the frame of Atangana-Baleanu derivative, *Fractal Fract.*, **5** (2021), 32. https://doi.org/10.3390/fractalfract5020032
41. A. Fernandez, I. Husain, Modified Mittag-Leffler functions with applications in complex formulae for fractional calculus, *Fractal Fract*., **4** (2020), 45. https://doi.org/10.3390/fractalfract4030045
42. A. O. Akdemir, A. Karaoğlan, M. A. Ragusa, E. Set, Fractional integral inequalities via Atangana-Baleanu operators for convex and concave functions, *J. Funct. Spaces*, **2021** (2021), 1055434. https://doi.org/10.1155/2021/1055434

43. K. A. Abro, M. H. Laghari, J. F. Gómez-Aguilar, Application of Atangana-Baleanu fractional derivative to carbon nanotubes based non-newtonian nanofluid: Applications in nanotechnology, *J. Appl. Comput. Mech.*, **6** (2020), 1260–1269.
44. A. G. M. Selvam, S. B. Jacob, Stability of Atangana-Baleanu fractional order differential equation with numerical approximation, *J. Phys.: Conf. Ser.*, **2070** (2021) 012086.
45. M. A. Elhagary, Effect of Atangana-Baleanu fractional derivative on a two-dimensional thermoviscoelastic problem for solid sphere under axisymmetric distribution, *Mech. Based Des. Struc.*, 2021. https://doi.org/10.1080/15397734.2021.1922288
46. A. Kilbas, H. M. Srivastava, J. J. Trujillo, *Theory and applications of fractional differential equations*, Elsevier Science, Amsterdam, The Netherlands, 2006.
47. A. Atangana, A. Akgul, K. M. Owolabi, Analysis of fractal fractional differential equations, *Alex. Eng. J.*, **59** (2020), 1117–1134. https://doi.org/10.1016/j.aej.2020.01.005
48. D. Y. Tzou, The generalized lagging response in small-scale and high-rate heating, *Int. J. Heat Mass Tran.*, **38** (1995), 3231–3240. https://doi.org/10.1016/0017-9310(95)00052-B
49. D. Y. Tzou, *Macro-to microscale heat transfer: The lagging behavior*, Taylor & Francis, New York, 2014.
50. A. E. Abouelregal, H. Ahmad, A modified thermoelastic fractional heat conduction model with a single-lag and two different fractional-orders, *J. Appl. Comput. Mech.*, **7** (2021), 1676–1686.
51. M. A. Ezzat, A. S. El-Karamany, S. M. Ezzat, Two-temperature theory in magneto-thermoelasticity with fractional order dual-phase-lag heat transfer, *Nuclear Eng. Design*, **252** (2012), 267–277. http://dx.doi.org/10.1016/j.nucengdes.2012.06.012
52. H. H. Sherief, M. N. Anwar, A problem in generalized thermoelasticity for an infinitely long annular cylinder, *Int. J. Eng. Sci.*, **26** (1988), 301–306. https://doi.org/10.1016/0020-7225(88)90079-1
53. G. Honig, U. Hirdes, A method for the numerical inversion of Laplace transforms, *J. Comput. Appl. Math.*, **10** (1984), 113–132. https://doi.org/10.1016/0377-0427(84)90075-X
54. A. E. Abouelregal, H. Ersoy, Ö. Civalek, Solution of Moore-Gibson-Thompson equation of an unbounded medium with a cylindrical hole, *Mathematics*, **9** (2021), 1536. https://doi.org/10.3390/math9131536

AIMS Press

© 2022 the Author(s), licensee AIMS Press. This is an open access article distributed under the terms of the Creative Commons Attribution License (http://creativecommons.org/licenses/by/4.0)